Journal of Process Control 118 (2022) 202–217

Contents lists available at ScienceDirect

Journal of Process Control

journal homepage: www.elsevier.com/locate/jprocont

Economic Oriented Dynamic Matrix Control of Wastewater Treatment Plants

Ioannis Kalogeropoulos [a], Alex Alexandridis [b], Haralambos Sarimveis [a,*]

[a] School of Chemical Engineering, National Technical University of Athens, Heroon Polytechneiou 9, Zografou, Athens, Greece
[b] Department of Electrical and Electronic Engineering, University of West Attica, Thivon 250, Aigaleo 12241, Greece

ARTICLE INFO

Article history:
Received 18 July 2021
Received in revised form 19 July 2022
Accepted 9 August 2022
Available online 19 September 2022

Keywords:
Economic model predictive control
Dynamic Matrix Control
Feedforward compensation
Wastewater Treatment Plant

ABSTRACT

Wastewater Treatment Plants (WWTPs) are industrial facilities, which are important for the protection of the environment, because they remove pollutants from wastewater, before it reaches natural bodies of water. WWTPs consist of complex physical, chemical, and biological energy-intensive processes, which are subject to significant disturbances and uncertainties, due to large variations in the load and quality of the influent. Rising energy prices and increasingly stringent effluent requirements have amplified the need of developing more efficient control schemes for WWTPs. In this paper a novel Economic Dynamic Matrix Control (EDMC) configuration is proposed for WWTPs, where the objective is to minimize the plant's operating costs in terms of energy savings, while maintaining the effluent quality within acceptable regulatory limits. The novelty of the proposed scheme lies in the combination of the standard Dynamic Matrix Control (DMC) methodology, with economic oriented control strategies. The EDMC predictive models are derived from the application of step tests on the COST/IWA Benchmark Simulation Model No. 1 (BSM1). Based on the BSM1 model, the proposed method is compared to standard Multiple Input–Multiple Output (MIMO) DMC controllers, to the default BSM1 control strategy and to other economic control methods, which have been proposed in the literature. The results illustrate that the proposed EDMC scheme is superior to alternative control strategies in terms of minimizing the energy consumption while, the effluent quality of the plant is maintained at acceptable levels.

1. Introduction

Water pollution is a major environmental issue that concerns both the scientific community and the society. More specifically, continuous deposition of nutrients and organic matter in water reservoirs may cause eutrophication and oxygen depletion, which lead to devastating consequences for both the flora and the fauna. In wastewater treatment plants (WWTPs), a combination of physical, chemical, and biological processes is applied to remove contaminants and impurities and convert wastewater into an effluent that can be returned to the water cycle. Although WWTPs are being used for several decades, their efficient operation and control remain a challenge due to the increasingly stringent limits enforced by regulators, the ongoing efforts to reduce the energy consumption and the complexity of the biological and biochemical phenomena involved in WWTP processes.

A review of the various strategies that have been proposed for the control of WWTPs has been presented in [1]. Due to the fact that aeration contributes from 45% to 75% to the overall energy cost in WWTPs [2], most of those approaches are focusing on aeration control. Many strategies, ranging from simple decentralized controllers to cascaded schemes are based on the classical Proportional–Integral (PI) architecture. In [3] a supervisory control structure is proposed, where the top control level, also referred as the cost controller, consists of three PI controllers, which are used to compute the most economical set-point for the decentralized controllers in the lower control level. In [4], it is illustrated that a decentralized control configuration, consisting of PI controllers, is capable of maintaining the process well within the regulatory limits at a small cost, in the presence of dynamic disturbances.

Model predictive control (MPC) is another approach that has been applied extensively for the control of WWTPs. MPC is an online optimal control method that optimizes the current and the future values of the manipulated variables based on the current state of the system, and future predictions, which are computed by a linear or nonlinear model of the plant. The objective function is typically a quadratic cost function, which penalizes deviations of the process states and input variables from their set-points. MPC is a popular technique due to its ability to control multivariable systems and to incorporate state and input constraints

* Corresponding author.
E-mail address: hsarimv@central.ntua.gr (H. Sarimveis).

https://doi.org/10.1016/j.jprocont.2022.08.006
0959-1524/

explicitly. In [5,6] a comparison between PI and MPC control strategies is performed. In [6], the existence of both MPC and PI controllers in one control configuration is examined. In [7] a procedure for tuning MPC parameters, namely the control horizon and the weights on state and input deviations, is described, based on H_∞ and l_1 norms of the closed loop transfer functions. In [8] a Dynamic Matrix Control (DMC) scheme is proposed, where truncated step responses are used to develop the linear model of the process. In [9], the authors presented an integrated MPC and monitoring system, which was applied to a WWTP in Lancaster, North England.

The aforementioned articles are representatives of the work that has been performed to date regarding PI and MPC control strategies with set-points, which are either fixed or are changing in a cascaded control approach. However, WWTPs are subject to very large fluctuations in their inlet flows and the existence of time periods at which the influent load might be very low. In such situations, the above-mentioned control schemes may result in larger than necessary energy consumptions, because they force the plant to reach unnecessary high set points (for example high levels of dissolved oxygen in aeration tanks). This issue has been addressed by applying multilayer hierarchical process control methodologies. According to this approach, in the upper real-time optimization (RTO) layer, the optimal set-points are computed, by optimizing a metric defining the operating profit or operating cost, with respect to up-to-date, steady state models of the process. The set-points are then used as targets in the lower supervisory control and regulatory control layers [10]. Although hierarchical control is a popular process control method with numerous successful implementations, it has some drawbacks. Given that optimizing over an accurate process model is of high importance for RTO to achieve a good performance, RTO has traditionally relied on complex, nonlinear models. On the contrary, the regulatory layer often relies on simple linear models, produced by traditional linearizing procedures. The discrepancies between the two models may result in operating points computed by RTO, that are unreachable from the regulatory layer. Moreover, the optimization procedure is performed only if the plant has reached a steady state. Since the process is subject to large and frequent fluctuations, waiting for the process to reach a steady-state may delay the computation of the new desired operating point. Thus, optimization may be performed only infrequently, resulting to poor performance of the controlled process. Dynamic RTO (D-RTO) alleviates these problems, using a dynamic model of the process, instead of steady-state models. In [10], applications of static RTO and D-RTO in WWTPs are presented and compared.

The idea of Economic MPC (EMPC) which incorporates economic cost functions in the MPC configuration has been proposed by many researchers [11–14]. EMPC has a similar structure to D-RTO, in that they both formulate dynamic optimization problems, which minimize an economic objective subject to a dynamic process model. EMPC approaches have been previously proposed for the control of WWTPs, using the Activated Sludge Model no. 1 (ASM1) as the predictive model of the plant [15]. In [16] an EMPC control scheme is presented, where a perfect match between the actual plant and the model is assumed. This assumption is however quite unrealistic, because in real-life plant operations, there are always present model uncertainties and discrepancies from the actual plant. To this end, reduction techniques have been employed for deriving simpler reduced order models [17]. In [18] a reduced nonlinear model, originally proposed in [10], is incorporated in an EMPC control strategy, which assumes perfect measurement of the state variables. Yet, knowledge of the full state of the system is not always possible [8], and measurements cannot be perfectly accurate, because of the noise that affects the feedback signals provided by the plant sensors.

In this paper, a novel linear Economic DMC (EDMC) control strategy is proposed for WWTPs, where the objective is to minimize the energy cost of the plant, while maintaining the effluent quality within acceptable regulatory limits. This goal is accomplished by incorporating a linear cost function in the formulation of the EDMC optimization problem, which reflects the main components contributing to the energy consumption of the plant; at the same time, effluent quality specifications are achieved by constraining the nitrate and nitrite oxygen and ammonium concentrations within upper and lower bounds in specific zones of the plant. This is the major contribution of the proposed approach as compared to standard DMC, where a quadratic objective function penalizes the discrepancies between predicted values of the controlled variables and the desired set points, but may lead to overcontrol of the plant, (i.e., more than necessary energy consumption), during periods of low pollutant influent loads. To the authors' best knowledge, this is the first time an economic formulation of DMC is presented. The other important properties of DMC, which render it a suitable control scheme for real life situations, are retained in the proposed EDMC approach; more specifically: 1. The linear prediction models involved in our EDMC approach are derived from the application of step tests, which are easily implementable on the actual plant. 2. The overall optimization problem is tractable, since it is a linear problem and can be solved efficiently using standard linear programming algorithms. 3. Modeling errors and uncertainties are handled efficiently, by estimating the error at each time instance and projecting it through the prediction horizon of the EDMC formulation. 4. Only the controlled variables need to be measured online and not the full state of the system.

The proposed EMPC approach is applied on the Benchmark Simulation Model no 1 (BSM) [19], a detailed dynamic model of WWTPs, which allows a fair comparison with alternative control strategies. More specifically, EDMC is compared with PI and MPC control schemes presented by Zeng and Liu [16], which were designed on the BSM1 model, assuming that the full state (145 state variables) is available. The proposed method is also compared to the MPC strategy described in [18], which as mentioned before, uses a reduced order model, but does not consider errors in state measurements.

The structure of the rest of the paper is as follows; in Section 2, a brief description of the BSM1 model is presented and the performance and cost indices concerning the operation of WWTPs are analyzed. In Section 3, the basic principles of the classical DMC algorithm are presented. In Section 4, the proposed EDMC methodology is described. Section 5 presents the predictive modeling development and validation results, closed-loop simulations, and comparison with alternative control strategies. Finally, Section 6 contains the conclusions of this work.

2. Description of the benchmark simulation model of wastewater treatment plants

All the control schemes designed in this work were tested on the BSM1 model (Fig. 1). BSM1 is a detailed model of a five-compartment biological reactor; the first two units (Unit 1 and 2) constitute the anoxic zone, where the denitrification process is performed, and the last three units (Units 3, 4 and 5) form the aerobic section, where the nitrification process occurs. Thus, the model combines the nitrification with denitrification processes in a configuration that is commonly used for achieving biological removal in full-scale WWTPs. Wastewater enters the anoxic section at a flow rate Q_0 and concentration Z_0, where Z denotes the different compounds involved in the wastewater treatment plant. The biological phenomena taking place in the biological reactor, are outlined using ASM1. Part of the stream

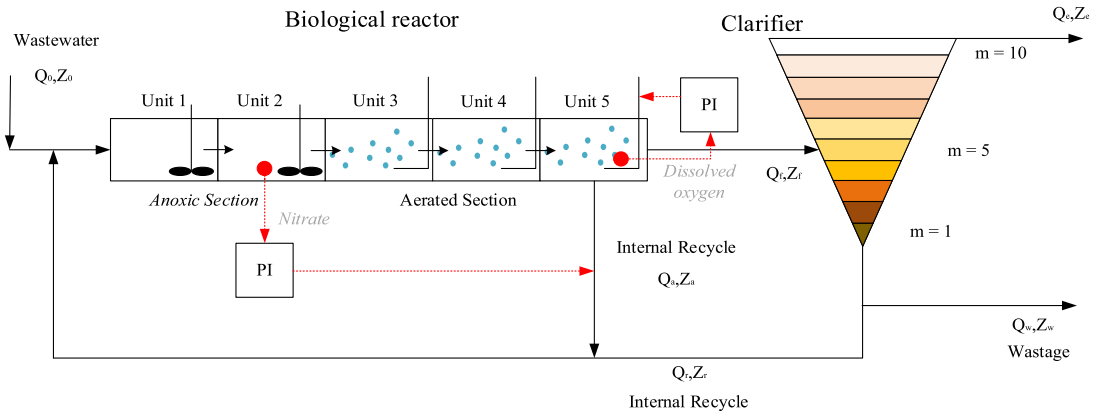

Fig. 1. General overview of the BSM no.1 plant.

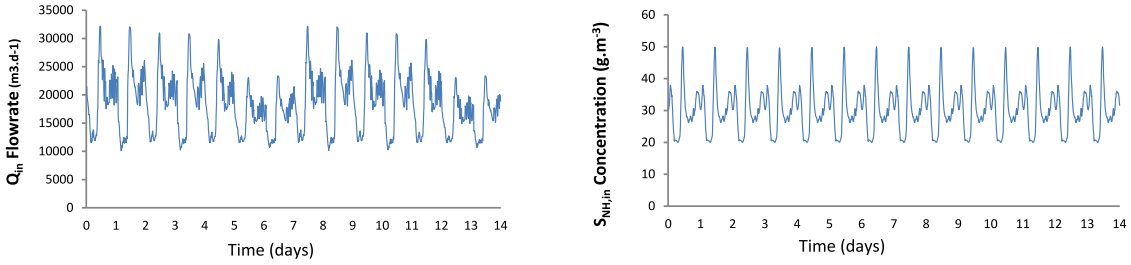

Fig. 2. Influent flow rate (a) and influent ammonium concentration (b) for the dry weather data set [19].

exiting the last aerated unit 5 is recycled to unit 1 at a flow rate Q_a and concentration Z_a, while the rest is feeding the secondary settler at a flow rate Q_f and concentration Z_f. The secondary settler is modeled as a ten-layer non-reactive unit. The sixth layer, counting from bottom to top as shown in Fig. 1, is the feed layer. From the upper layer of the settler, the processed water is removed at a flow rate Q_e and concentration Z_e. From the bottom layer of the settler the underflow stream at a flow rate Q_u and concentration Z_u is partially returned to unit 1 (the second recycling stream) at flow rate Q_r and concentration Z_r, while the rest is withdrawn at flow rate Q_w and concentration Z_w.

Table 1 contains the BSM1 model parameters as they are provided by [19]. The default BSM1 control scheme consists of two PI control loops; the first loop controls the nitrite and nitrate nitrogen concentration in the second anoxic tank ($S_{NO,2}$) using the internal recycling stream (Q_a) as the manipulated variable. The second loop controls the dissolved oxygen concentration in the last aerated tank ($S_{O,5}$) by manipulating the oxygen transfer coefficient in the last aerated tank (K_La_5). Table 2 depicts the gains (K), the integral time constants (T_i) and the anti-windup time constants (T_t) of the two default PI controllers, and the respective set-point values.

Three different dynamic influent data sets are provided by the IWA Task Group [20] in terms of ASM1 state variables, representing different weather conditions. The first set corresponds to a typical dry period, the second one represents a long rain event, and the third set combines dry weather conditions with two different storm events. The duration of all influent data sets spans 14 days. Table 3 presents the constant influent profile alongside the steady state values for all five compartments of the biological reactor. In Fig. 2, the profiles of influent flow rate and influent ammonium nitrogen concentration for the dry weather conditions are provided.

Table 1
BSM no.1 model parameters.

Parameter	Value
Volume (V_i) i = 1,2	1000 (m^3)
Volume (V_i) i = 3,4,5	1333 (m^3)
Q_w	385 (m^3 d^{-1})
Q_r	18 846 (m^3 d^{-1})
Volume of settler	6000 (m^3)
Area of settler	1500 (m^3)
Height of each layer	0.4 (m)
Number of layers	10
$K_La_{3,4}$	240 (d^{-1})

3. Dynamic matrix control

3.1. Standard dynamic matrix control

The concept of MPC was first introduced by [21] in late '70s. In particular, the DMC algorithm [22] was proposed by two Shell engineers and is the simplest and, at the same time, the most widespread MPC algorithm in the industry. The values of the optimized future manipulated variables are derived from the minimization of an appropriately defined quadratic objective function containing both the deviation of the predicted outputs from a desired reference and the variation of the manipulated inputs. The model of the process which is used for the prediction of the future behavior of the output variables is usually derived from step or impulse response tests which are applied on the

Table 2
Default PI control strategy parameters [19].

Controlled variable	PI-Parameter				Manipulated variable
	K	T_i	T_t	Set point	
$S_{NO,2}$ (g N m^{-3})	10 000 m^3 d^{-1} (g N m^{-3})$^{-1}$	0.025 d	1.015 d	1 g N m^{-3}	Q_a
$S_{O,5}$ (g(−COD) m^{-3})	25 d^{-1} (g(−COD) m^{-3})$^{-1}$	0.002 d	0.001 d	2 g(−COD) m^{-3}	K_La_5

Table 3
Biological reactor constant influent profile and steady state values for the five compartments [19].

	Description	Influent	Unit 1	Unit 2	Unit 3	Unit 4	Unit 5
S_I (g COD m^{-3})	Soluble inert organic matter	30	30	30	30	30	30
S_S (g COD m^{-3})	Readily biodegradable substrate	69.5	2.81	1.46	1.15	0.995	0.889
X_I (g COD m^{-3})	Particulate inert organic matter	51.2	1149	1149	1149	1149	1149
X_S (g COD m^{-3})	Slowly biodegradable substrate	202.32	82.1	76.4	64.9	55.7	49.3
$X_{B,H}$ (g COD m^{-3})	Active heterotrophic biomass	28.17	2552	2553	2557	2559	2559
$X_{B,A}$ (g COD m^{-3})	Active autotrophic biomass	0	148	148	149	150	150
X_P (g COD m^{-3})	Particulate products arising from biomass decay	0	449	450	450	451	452
S_O (g −COD m^{-3})	Oxygen	0	0.0043	0.0000631	1.72	2.43	0.491
S_{NO} (g N m^{-3})	Nitrate and nitrite nitrogen	0	5.37	3.66	6.54	9.3	10.4
S_{NH} (g N m^{-3})	NH_4^+ + NH_3 nitrogen	31.56	7.92	8.34	5.55	2.97	1.73
S_{ND} (g N m^{-3})	Soluble biodegradable organic matter	6.95	1.22	0.882	0.829	0.767	0.688
X_{ND} (g N m^{-3})	Particulate biodegradable organic nitrogen	10.59	5.28	5.03	4.39	3.88	3.53
S_{ALK} (mol m^{-3})	Salinity	7	4.93	5.08	4.67	4.29	4.13
X (g SS m^{-3})	Sludge	–	3285	3282	3278	3274	3270
Q (m^3 d^{-1})	Flow	18 446	92 230	92 230	92 230	92 230	92 230

actual plant, or on a detailed model of the system. The basic principles that govern the DMC algorithm are well established in the literature [23–25], so only a brief description of the method is presented here.

In this work, step response models around a steady-state are developed, in the form of:

$$y(t) = \sum_{i=1}^{\infty} g_i \Delta u(t-i) \tag{3.1}$$

where $y(t)$ denotes the output deviation variable (i.e., the full value of the output variable minus the value at the steady state), Δu is the incremental change of the manipulated variable u between two consecutive discrete time instances, $\Delta u(t-i) = u(t-i) - u(t-i-1)$ and g_i is the step response coefficient at time instant i. The prediction of the output value for a future time instant k is given by:

$$\begin{aligned}\hat{y}(t+k|t) &= \sum_{i=1}^{\infty} g_i \Delta u(t+k-i|t) + d_{unm}(t+k|t) \\ &= \sum_{i=1}^{k} g_i \Delta u(t+k-i|t) + \sum_{i=k+1}^{\infty} g_i \Delta u(t+k-i|t) \\ &\quad + d_{unm}(t+k|t)\end{aligned} \tag{3.2}$$

where, $d_{unm}(t+k|t)$ is the term representing the prediction of unmeasured disturbance at time instant k. In classical DMC, this term is set equal to the current measurement error, thus:

$$\begin{aligned}\hat{y}(t+k|t) &= \sum_{i=1}^{k} g_i \Delta u(t+k-i|t) + \sum_{i=k+1}^{\infty} g_i \Delta u(t+k-i|t) \\ &\quad + y_m(t) - y_{ss} - \sum_{i=1}^{\infty} g_i \Delta u(t-i) \\ &= \sum_{i=1}^{k} g_i \Delta u(t+k-i|t) + \sum_{i=1}^{\infty} g_{k+i} \Delta u(t-i) + y_m(t) \\ &\quad - y_{ss} - \sum_{i=1}^{\infty} g_i \Delta u(t-i) \\ &= \sum_{i=1}^{k} g_i \Delta u(t+k-i|t) + y_m(t) - y_{ss} + \sum_{i=1}^{\infty} (g_{k+i} - g_i) \Delta u(t-i) \\ &= \sum_{i=1}^{k} g_i \Delta u(t+k-i|t) + f(t+k)\end{aligned} \tag{3.3}$$

where, y_{ss} is the steady state value, $y_m(t)$ is the current measurement of the output variable, taken from the real plant, and $f(t+k)$ is the free response of the system. Assuming only open loop asymptotically stable systems, i.e., systems which reach a steady state over a finite time horizon l_{pin}, the free response of the system takes the following form:

$$f(t+k) = y_m(t) - y_{ss} + \sum_{i=1}^{l_{pin}} (g_{k+i} - g_i) \Delta u(t-i) \tag{3.4}$$

The predictions of the output variables along the prediction horizon N_p can be grouped in a vector that is related to the vector that contains the future incremental changes of the manipulated variables through the following equation:

$$\begin{bmatrix} \hat{y}(t+1|t) \\ \vdots \\ \hat{y}(t+N_p|t) \end{bmatrix} = A * \begin{bmatrix} \Delta u(t) \\ \vdots \\ \Delta u(t+N_c) \end{bmatrix} + \begin{bmatrix} f(t+1) \\ \vdots \\ f(t+N_p) \end{bmatrix} \tag{3.5}$$

where the symbol N_c denotes the control horizon, beyond which no control moves are allowed. The length of the control horizon N_c should be less than or equal to the prediction horizon N_p. A is the dynamic matrix of the system, which in the case of a Single Input–Single Output (SISO) system has dimensions $N_p \times N_c$ and is formulated as follows, based on the coefficients of the

step-response model:

$$A = \begin{bmatrix} g_1 & 0 & \dots & 0 \\ g_2 & g_1 & \dots & 0 \\ \vdots & \vdots & \ddots & \vdots \\ g_{N_c} & g_{N_c-1} & \dots & g_1 \\ \vdots & \vdots & & \vdots \\ g_{l_{pin}} & g_{l_{pin}-1} & \dots & g_{l_{pin}-N_c+1} \\ \vdots & \vdots & & \vdots \\ g_{l_{pin}} & g_{l_{pin}} & \dots & g_{l_{pin}} \end{bmatrix} \tag{3.6}$$

In the case of Multiple Input–Multiple Output (MIMO) systems, the dynamic matrix A is formulated as follows:

$$A = \begin{bmatrix} A_{1,1} & \dots & A_{1,n_{in}} \\ \vdots & A_{i,j} & \vdots \\ A_{n_{out},1} & \dots & A_{n_{out},n_{in}} \end{bmatrix} \tag{3.7}$$

where n_{in} is the number of manipulated variables and n_{out} is the number of controlled variables; each matrix $A_{i,j}$ has dimensions $N_p \times N_c$ and is constructed like matrix A in Eq. (3.6), using the coefficients of the step response model between the manipulated variable j and the controlled variable i.

Disturbances that can be estimated with high confidence during the prediction horizon may be included in the prediction model as additional input variables, which however, cannot be manipulated [23]. In this case, the prediction model is modified as follows:

$$\hat{y}(t+k|t) = \sum_{i=1}^{k} g_i \Delta u(t+k-i|t) + \sum_{i=1}^{k} g_i' \Delta d(t+k-i|t) + f(t+k) \tag{3.8}$$

where the free response of the system is now represented by the following form:

$$f(t+k) = y_m(t) - y_{ss} + \sum_{i=1}^{l_{pin}} (g_{k+i} - g_i) \Delta u(t-i) + \sum_{i=1}^{l_{pin}} \left(g_{k+i}' - g_i'\right) \Delta d(t-i) \tag{3.9}$$

In Eq. (3.8) Δd is the incremental change of the measured disturbance d between two consecutive discrete time instances, $\Delta d(t-i) = d(t-i) - d(t-i-1)$ and g_i' is the corresponding step response coefficient at time instant i. The vector containing the predictions of the output variables along the prediction horizon N_p is now described by the following equation:

$$\begin{bmatrix} \hat{y}(t+1|t) \\ \vdots \\ \hat{y}(t+N_p|t) \end{bmatrix} = A * \begin{bmatrix} \Delta u(t) \\ \vdots \\ \Delta u(t+N_c) \end{bmatrix} + B * \begin{bmatrix} \Delta d(t) \\ \vdots \\ \Delta d\left(t+N_p\right) \end{bmatrix} + \begin{bmatrix} f(t+1) \\ \vdots \\ f\left(t+N_p\right) \end{bmatrix} \tag{3.10}$$

In the case of a system with one controlled variable and one measured disturbance, B is a matrix with dimensions $N_p \times N_p$ that contains the step response coefficients corresponding to the measured disturbance:

$$B = \begin{bmatrix} g_1' & 0 & \dots & 0 \\ g_2' & g_1' & \dots & 0 \\ \vdots & \vdots & \ddots & \vdots \\ g_{N_p}' & g_{N_p-1}' & \dots & g_1' \end{bmatrix} \tag{3.11}$$

In the case of systems with multiple outputs and/or disturbances, the matrix B takes the following form:

$$B = \begin{bmatrix} B_{1,1} & \dots & B_{1,n_d} \\ \vdots & B_{i,j} & \vdots \\ B_{n_{out},1} & \dots & B_{n_{out},n_d} \end{bmatrix} \tag{3.12}$$

where n_d is the number of measured disturbances; each matrix $B_{i,j}$ has dimension $N_p \times N_p$ and is constructed like matrix B in Eq. (3.11), using the coefficients of the step response model between the measured disturbance j and the controlled variable i.

According to the classical DMC theory, the optimization problem depicted in Box I is formulated and solved at each discrete time instant t.

The objective function in Eq. (3.13), contains the deviations of the predicted process outputs from the desired set point and the incremental changes on the future values of the manipulated variables Δu. The symbol $\|\cdot\|$ denotes the quadratic norm, N_p and N_c refer to the prediction horizon and the control horizon, respectively, Q and R are positive definite matrices used for balancing the two terms in the objective function, and u_{min}, u_{max}, y_{min} and y_{max} are vectors defining the minimum and maximum bounds on the manipulated and the controlled variables, respectively. From the optimal input trajectory $u^* = [u_1^*, \dots, u_{N_c}^*]$, only the first element is actually applied to the plant, and the optimization problem defined in Eq. (3.13) is reformulated and solved again at the next time instant.

Due to large variations in the dynamic influent profiles in terms of both flow rates and compositions, there exist situations when the hard output constraints imposed on the controlled variables cannot be satisfied during the entire prediction horizon, and this leads to infeasibility issues in the solution of the DMC optimization problem (3.13). This issue is addressed by substituting the hard constraints on the future predictions of the controlled variables by soft constraints, using non-negative variables $\varepsilon_{min}(t+k)$, $\varepsilon_{max}(t+k)$, $k = 1..N_p$, which take positive values only when upper or lower bounds are violated [26]. In this case, the formulation of the DMC optimization problem is modified as in Box II, where, ρ_{min} and ρ_{max} are weights used to penalize soft constraint violations and ε_{min}, ε_{max} are vectors of appropriate dimensions containing the slack variables, that correspond to the minimum and maximum bounds imposed on the controlled variables.

The DMC control schemes that were developed in this work for the control of WWTPs, considered three controlled outputs, namely the nitrate and nitrite nitrogen concentration in the second tank $S_{NO,2}$, the ammonium concentration in the last aerated reactor $S_{NH,5}$, and the nitrate and nitrite concentration in the last aerated reactor, denoted by $S_{NO,5}$. Effluent ammonium concentration $S_{NH,eff}$ could also be a choice, however as it is mentioned in [4], "as a means to improve control of $S_{NH,eff}$, it is more prudent to control $S_{NH,5}$ instead, because the settler can serve as a low-pass filter to damp large dynamic variations in $S_{NH,eff}$. Moreover, $S_{NH,5}$ is not less of an active constraint than $S_{NH,eff}$ is". In addition, by selecting $S_{NH,5}$ as a control variable, we are avoiding the large time delays, which occur in the settler. For dynamic simulation purposes, three B_0 class (gas sensitive plus normal filtration)

$$\min_{\Delta u(k),\Delta u(k+1),\ldots,\Delta u(k+N_c)} \sum_{k=1}^{N_p} \left\| \hat{y}\,(t+k|t) - y_{sp} \right\|_Q^2 + \sum_{k=0}^{N_c} \left\| \Delta u(t+k) \right\|_R^2$$

$$s.t. \quad \begin{bmatrix} \hat{y}\,(t+1|t) \\ \vdots \\ \hat{y}(t+N_p|t) \end{bmatrix} = A* \begin{bmatrix} \Delta u\,(t) \\ \vdots \\ \Delta u\,(t+N_c) \end{bmatrix} + B* \begin{bmatrix} \Delta d\,(t) \\ \vdots \\ \Delta d\left(t+N_p\right) \end{bmatrix} + \begin{bmatrix} f\,(t+1) \\ \vdots \\ f\left(t+N_p\right) \end{bmatrix} \tag{3.13}$$

$$u_{min} \le u\,(t+k) \le u_{max}, \quad k = 1..N_c$$

$$y_{min} \le y\,(t+k|t) \le y_{max}, \quad k = 1..N_p$$

$$\Delta u\,(t+k) = u\,(t+k) - u\,(t+k-1)\,, \quad k = 1..N_c$$

Box I.

$$\min_{\Delta u(k),\Delta u(k+1),\ldots,\Delta u(k+N_c)} \sum_{k=1}^{N_p} \left\| \hat{y}\,(t+k|t) - y_{sp} \right\|_Q^2 + \sum_{k=0}^{N_c} \left\| \Delta u\,(t+k) \right\|_R^2 + \rho_{min} \sum_{k=1}^{N_p} \sum_{i=1}^{n_{out}} \varepsilon_{min,i}\,(t+k) + \rho_{max} \sum_{k=1}^{N_p} \sum_{i=1}^{n_{out}} \varepsilon_{max,i}\,(t+k)$$

$$s.t. \quad \begin{bmatrix} \hat{y}\,(t+1|t) \\ \vdots \\ \hat{y}(t+N_p|t) \end{bmatrix} = A* \begin{bmatrix} \Delta u\,(t) \\ \vdots \\ \Delta u\,(t+N_c) \end{bmatrix} + B* \begin{bmatrix} \Delta d\,(t) \\ \vdots \\ \Delta d\left(t+N_p\right) \end{bmatrix} + \begin{bmatrix} f\,(t+1) \\ \vdots \\ f\left(t+N_p\right) \end{bmatrix} \tag{3.14}$$

$$u_{min} \le u\,(t+k) \le u_{max}, \quad k = 1..N_c$$

$$y_{min} - \varepsilon_{min}\,(t+k) \le \hat{y}\,(t+k|t) \le y_{max} + \varepsilon_{max}\,(t+k)\,, \quad k = 1..N_p$$

$$\varepsilon_{min}(t+k), \varepsilon_{max}(t+k) \ge 0, \quad k = 1..N_p$$

$$\Delta u\,(t+k) = u\,(t+k) - u\,(t+k-1)\,, \quad k = 1..N_c$$

Box II.

Table 4
Control configuration description.

Model dimension ($n_{out} \times n_{in}$)	Controlled outputs	Manipulated inputs	Set points	Measured disturbances
3×2	$\begin{bmatrix} S_{NO,2} \\ S_{NH,5} \\ S_{NO,5} \end{bmatrix}$	$\begin{bmatrix} Q_a \\ K_L a_5 \end{bmatrix}$	$\begin{bmatrix} S_{NO,2}^{s.p.} = 3.66 \text{ g N m}^{-3} \\ S_{NH,5}^{s.p.} = 1.73 \text{ g N m}^{-3} \\ S_{NO,5}^{s.p.} = 10.42 \text{ g N m}^{-3} \end{bmatrix}$	$\begin{bmatrix} Q_{in} \\ S_{NH,in} \end{bmatrix}$

sensors were used, with a measurement range $0 - 20$ g N m^{-3} and measurement noise $\delta = 0.5$ g N m^{-3}, one for each controlled output, as it is recommended in [19].

In all control schemes presented in this work, two manipulated variables were used, namely the internal recirculation flow rate Q_a and the oxygen transfer coefficient in the last aerated tank $K_L a_5$. Two measured disturbances were considered: The influent flow rate Q_{in} and the influent ammonium concentration $S_{NH,in}$. Both disturbances can be predicted with high accuracy in real life WWTPs, using historical information for the same season of operation and considering the weather forecast. The controlled outputs, manipulated inputs, set points and measured disturbances are summarized in Table 4.

The steady state suggested by [19], was used as a basis to perform the step tests in Section 5.1 and derive the step-response predictive models. Table 5 presents the steady state values for the manipulated and the controlled variables and the measured disturbances; it also presents the constraints that were imposed on the manipulated and controlled variables in the formulation of the DMC optimization problem. Upper bounds on the manipulated variables are due to the capacities of the respective pumps and were selected in accordance with [19]. As far as the controlled variables are concerned, a low bound other than zero (0) was imposed only in the case of $S_{NO,2}$, as recommended by [4]. The upper bound on $S_{NH,eff}$ proposed in [19] was used in this work as an upper bound for $S_{NH,5}$. The upper limit on $S_{NO,5}$ was selected so that it offers a good compromise in terms of effluent quality and operation cost. Lower bounds on the summation $S_{NH,5}+S_{NO,5}$, recommended in [5,27], led to inferior performances.

3.2. Economic dynamic matrix control

The proposed EDMC methodology is different to the standard DMC method only with respect to the objective function, which is now linear and includes the energy cost of the last energy tank, the pumping energy cost of the recirculation flow, and penalties in the form of slack variables, when effluent concentrations are not within acceptable limits: the formulation of the EDMC optimization problem is shown in Box III.

The two cost terms considered in Eq. (3.15) are the aeration energy consumed in the last aerated tank $AE_5\,(t+k)$ (kWh) and the internal recirculation pumping energy, $PE_{Q_a}\,(t+k)$ (kWh). The equations describing the two cost items are given below:

$$AE_5\,(t+k) = \frac{S_{O,sat} * V_5}{1800} K_L a_5\,(t+k)\,, k = 1..N_p \tag{3.16}$$

Table 5
Steady state values and upper and lower bounds on process variables.

Manipulated input	Steady-state value	Minimum value	Maximum value
Q_a	55 338 (m^3 d^{-1})	0 (m^3 d^{-1})	92 230 (m^3 d^{-1})
K_La_5	84 (d^{-1})	20 (d^{-1})	240 (d^{-1})
Controlled output			
$S_{NO,2}$	3.66 (g N m^{-3})	1 (g N m^{-3})	5 (g N m^{-3})
$S_{NH,5}$	1.73 (g N m^{-3})	0	4 (g N m^{-3})
$S_{NO,5}$	10.42 (g N m^{-3})	0	11 (g N m^{-3})
Measured disturbance			Steady state value
Q_{in}			18 446 (m^3 d^{-1})
$S_{NH,in}$			31.56

$$
\begin{aligned}
&\min_{\Delta u(k),\Delta u(k+1),\ldots,\Delta u(k+N_p)} \left[\begin{array}{c} R_1\left(\frac{w_1}{N_p}\sum_{k=1}^{N_p} AE_5\,(t+k)+\frac{w_2}{N_p}\sum_{k=1}^{N_p} PE_{Q_a}\,(t+k)\right)+ \\ R_2\left(\rho_{min}\sum_{k=1}^{N_p}\sum_{i=1}^{n_{out}}\varepsilon_{min,i}\,(t+k)+\rho_{max}\sum_{k=1}^{N_p}\sum_{i=1}^{n_{out}}\varepsilon_{max,i}\,(t+k)\right)\end{array}\right] \\
&s.t.\quad \begin{bmatrix}\hat{y}\,(t+1|t)\\ \vdots \\ \hat{y}(t+N_p|t)\end{bmatrix} = A*\begin{bmatrix}\Delta u\,(t)\\ \vdots \\ \Delta u\,(t+N_c)\end{bmatrix} + B*\begin{bmatrix}\Delta d\,(t)\,v\\ \vdots \\ \Delta d\left(t+N_p\right)\end{bmatrix} + \begin{bmatrix} f\,(t+1)\\ \vdots \\ f\left(t+N_p\right)\end{bmatrix} \\
&AE_5\,(t+k) = \frac{S_{O,sat}*V_5}{1800}K_La_5\,(t+k)\,,\quad k=1..N_p \\
&PE_{Q_a}\,(t+k) = 0.004Q_a\,(t+k)\,,\quad k=1..N_p \\
&u_{min}\le u\,(t+k)\le u_{max},\qquad k=1..N_p \\
&y_{min}-\varepsilon_{min}\,(t+k)\le\hat{y}\,(t+k|t)\le y_{max}+\varepsilon_{max}\,(t+k)\,,\quad k=1..N_p \\
&\varepsilon_{min}(t+k),\,\varepsilon_{max}(t+k)\ge 0,\quad k=1..N_p \\
&\Delta u\,(t+k) = u\,(t+k)-u\,(t+k-1)\,,\quad k=1..N_p
\end{aligned}
\tag{3.15}
$$

Box III.

$$PE_{Q_a}\,(t+k) = 0.004Q_a\,(t+k)\,,\, k=1..N_p \tag{3.17}$$

where $S_{O,sat}$ is the saturation concentration for oxygen, which is equal to 8 g m^{-3}. Both cost items are linear with respect to the decision variables $K_La_5\,(t+k)$ and $Q_a\,(t+k)$.

In Eq. (3.15), the weights R_1 and R_2 are selected to balance the two control objectives, while ρ_{min} and ρ_{max} are used to penalize soft constraint violations. The constraints in the formulation of the EDMC optimization problem are exactly the same with the constraints appearing in the standard DMC configuration (Eq. (3.14) and Table 5).

The implementation strategy of EDMC is identical to the receding horizon strategy of conventional DMC. At each sampling instance, the EDMC controller receives real-time measurements from the process sensors regarding the controlled variables and solves the linear optimization problem defined by the economic objective function and the constraints in Eq. (3.15). The result of the optimization problem is the optimal input trajectory over the prediction horizon. The first control action is actually implemented by the actuators, and the optimization problem is reformulated and resolved at the next sampling period.

4. Performance indicators

Several performance indicators were employed for validating the proposed control schemes and comparing them with other control configurations. Regarding the quality of the effluent stream, which leaves the process from the settler's upper layer, the following performance metrics were used:

- The mean values of effluent ammonia nitrogen and nitrate and nitrite nitrogen concentrations over the evaluation period, denoted by $\bar{S}_{NH,eff}$ and $\bar{S}_{NO,eff}$, as suggested by [19].
- The Effluent Quality (EQ) index, described in [19], which is presented in the following equation:

$$EQ = \frac{1}{1000T}\int_{t_o}^{t_f}\left(2*SS_{eff}\,(t)+COD_{eff}\,(t)+30*S_{Nkj,eff}\,(t)\right. \\ \left.+10*S_{NO,eff}\,(t)+2*BOD_{eff}\,(t)\right)*Q_{eff}\,(t)\,dt \tag{4.1}$$

  In Eq. (4.1), SS_{eff} is the effluent suspended solids concentration, COD_{eff} is the effluent Chemical Oxygen Demand (COD), $S_{Nkj,eff}$ is the effluent Kjeldahl nitrogen concentration, $S_{NO,eff}$ is the effluent nitrate and nitrite nitrogen concentration, BOD_{eff} is the effluent Biochemical Oxygen Demand (BOD), Q_{eff} is the effluent flow rate and $T = t_f - t_0$ is the evaluation time period (in days).
- The time periods when the effluent constraints on TN_{eff} and $S_{NH,eff}$, shown in Table 6, are violated. The total effluent nitrogen concentration TN_{eff} is defined as the summation of effluent Kjeldahl nitrogen concentration and the effluent nitrate and nitrite nitrogen ($S_{NO,eff}$) concentration. The effluent quality upper bounds in Table 6 are in accordance with [19].

Table 6
Effluent quality limit values.

Variable	Upper bound
TN_{eff}	<18 g N m^{-3}
$S_{NH,eff}$	<4 g N m^{-3}

Regarding the operational cost of the WWTP, the following performance indicators are used for evaluation and comparison purposes:

- The daily Cost Index (CI) which is defined as the summation of the aeration energy in the last aerated tank and the recirculation pumping energy, averaged over the evaluation period:

$$AE_5 = \frac{1}{T}\int_{t_o}^{t_f} AE_5\,(t)\,dt, \quad PE_{Q_a} = \frac{1}{T}\int_{t_o}^{t_f} PE_{Q_a}\,(t)\,dt, \qquad CI = AE_5 + PE_{Q_a} \tag{4.2}$$

- The daily Overall Cost Index (OCI) defined in [19], which is computed as a weighted summation of the total aeration energy AE, the total pumping energy PE, the total sludge production SP, the total consumption of external carbon source EC and the total mixing energy ME of the BSM1 plant, over the evaluation period:

$$OCI = \frac{1}{T}\int_{t_o}^{t_f} (AE\,(t) + PE\,(t) + 5\cdot SP\,(t) + 3\cdot EC\,(t) + ME\,(t))\,dt \tag{4.3}$$

5. Simulation results

5.1. Step responses & model derivation

Step tests were performed on all manipulated variables and measured disturbances, using the BSM1 model and starting from the steady state values, which were presented in Table 5. In all step tests, the step size was +10% of the steady state value. A sampling period of $T_s = 15$ min was used for deriving the model coefficients.

Figs. 3 to 5 present the responses of the output variables $S_{NH,5}$, $S_{NO,2}$ and $S_{NO,5}$, which are reaching new steady state values after 96 time periods of 15 min. Therefore, the system is open loop stable and step response models can be derived using $l_{pin} = 96$ coefficients. These coefficients, $g_i^{j,l}$, were obtained for each combination of controlled output $j = 1, \ldots, 3$ and manipulated input $l = 1, 2$ at each time instant $i = 1, \ldots, l_{pin}$ as follows:

$$g_i^{j,l} = \frac{y_i^j - y_{s.s}^j}{u_f^l - u_{s.s}^l} \tag{5.1}$$

In the above equation $y_{s.s}^j$ is the steady-state value of control output j, $u_{s.s}^l$ is the steady-state value of manipulated input l and u_f^l is the final value of manipulated input l after the step response.

The coefficients for the measurable disturbances were derived in a similar fashion. In Figs. 6 to 8 step responses for $S_{NH,5}$, $S_{NO,2}$ and $S_{NO,5}$ to both the measurable disturbances are shown; the coefficients $g_i^{\prime j,m}$ for each combination of controlled output $j = 1, 2, 3$ and measured disturbance $m = 1, 2$, were computed as follows:

$$g_i^{\prime j,m} = \frac{y_i^j - y_{s.s}^j}{d_f^m - d_{s.s}^m} \tag{5.2}$$

where, $y_{s.s}^j$ is the steady-state value of control output j, $d_{s.s}^m$ is the steady-state value on measured disturbance m and d_f^m is the final value of measured disturbance m after the step response.

Table 7
Coefficients of determination (R^2) corresponding to step-response models with 24,48 or 96 coefficients.

Controlled variable	R^2		
	$l_{pin} = 24$	$l_{pin} = 48$	$l_{pin} = 96$
$S_{NH,5}$	0.82	0.83	0.99
$S_{NO,2}$	0.75	0.82	0.84
$S_{NO,5}$	0.34	0.53	0.83

Table 8
DMC and EDMC control schemes.

Controller	Step response horizon (l_{pin})	Remarks
DMC_3by2_48	48	Classic DMC
DMC_3by2_96	96	Classic DMC
EDMC_3by2_48	48	Economic DMC
EDMC_3by2_96	96	Economic DMC

5.2. Model validation

The prediction accuracy of the step response models employed in the DMC or EDMC configurations is important for the successful performance of the control algorithms. This subsection examines if consideration of larger sampling intervals, can produce step response models of acceptable prediction accuracies. More specifically, in addition to the base case, which uses $T_s = 15$ min, we derived step response models with 48 and 24 coefficients using sampling intervals of 30 min and 60 min, respectively.

Fig. 9 provides a comparison between the model predictions of the step response models with 96, 48 or 24 coefficients and the actual responses of the output variables $S_{NO,2}$ and $S_{NO,5}$ corresponding to the 8th day of the dry weather data set. The coefficients of determination, (R^2 values) for all three output variables are shown in Table 7.

Table 7 illustrates that the step response models with 96 coefficients lead to high R^2 values for all the controlled variables. The models having 48 coefficients are clearly less accurate, but their R^2 values are still acceptable. Therefore, these models will be considered as alternative predictive models in the formulations of the DMC and EDMC algorithms in the next subsection. The models that contain only 24 coefficients have poor correlation with the actual responses and will not be studied further.

5.3. Controller design and results

This subsection presents and compares the results of the DMC and EDMC algorithms on the problem of controlling the BSM1 WWTP model. For both DMC and EDMC methods, we used the two manipulated variables and the three controlled variables shown in Table 5, we included the effect of the measured disturbance as shown in Eq. (3.8), and we employed the step response models with 48 or 96 coefficients, presented in Section 5.2. This led to the design of four control configurations, which are shown in Table 8. In all simulations that are presented in this subsection, the BSM1 model played the role of the real plant, which means that the control actions were applied on the BSM1 model and the $y_m\,(t)$ values used in Eq. (3.9) were the output values of the BSM1 model. Therefore, the errors between the BSM1 model and the predictive step response models are introduced into the DMC and EDMC algorithms via Eq. (3.9).

The tuning parameters (weighting matrices Q and R in DMC, R_1, R_2, w_1 and w_2 in EDMC and ρ_{min} and ρ_{max} used in both DMC and EDMC control formulations) were selected by trial and error to achieve a successful compromise between the cost and constraint violation terms. Their values are depicted in Table 9.

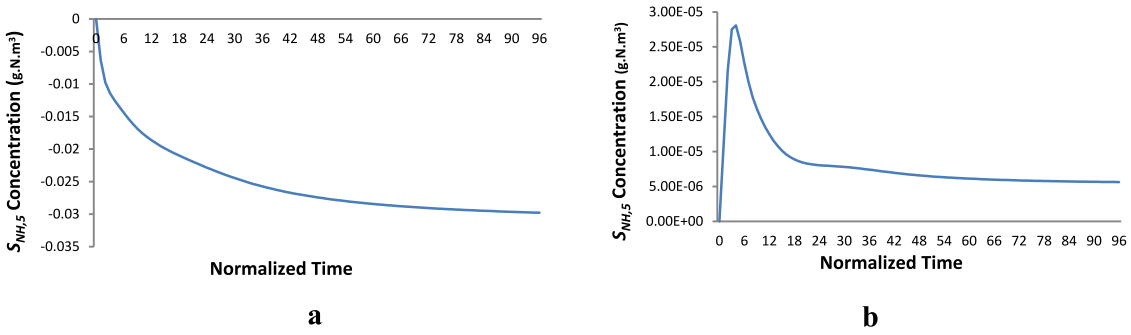

Fig. 3. $S_{NH,5}$ step responses to oxygen transfer coefficient (a) and internal recirculation flow rate (b).

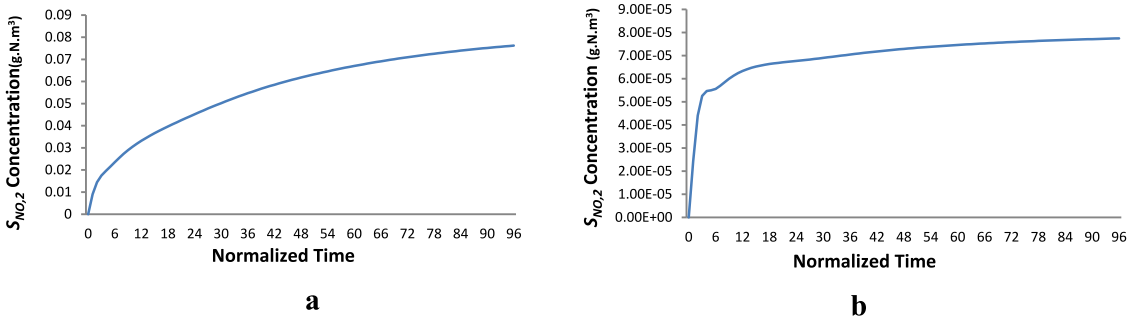

Fig. 4. $S_{NO,2}$ step responses to oxygen transfer coefficient (a) and internal recirculation flow rate (b).

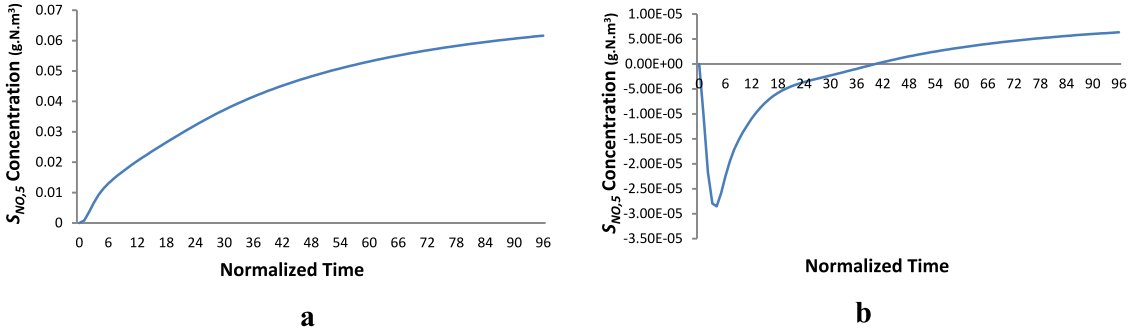

Fig. 5. $S_{NO,5}$ step responses to oxygen transfer coefficient (a) and internal recirculation flow rate (b).

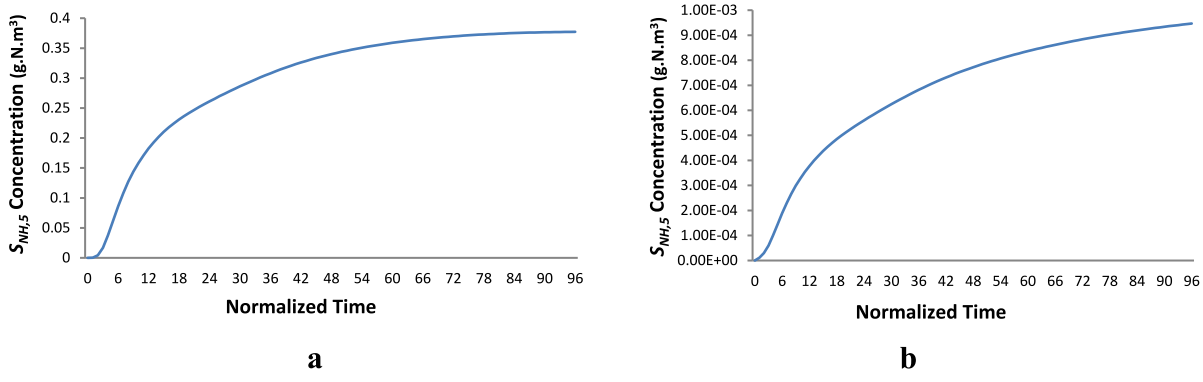

Fig. 6. $S_{NH,5}$ step responses to influent flow rate (a) and influent ammonium concentration (b).

All simulations were performed as suggested by Alex et al. [19], i.e. first a closed loop stabilization period for 150 days was completed under constant influent conditions (first two columns of Table 3) and assuming that no noise is added on the measurements. During the stabilization period, the same controller was used in all simulations, namely the DMC_3by2_96, so that the same initial conditions, presented in Table 3, were used by all the control schemes. After the stabilization period, two closed loop dynamic simulation periods of seven (7) days each, were performed. The first one was considered as a dynamic stabilization period, while the latter was used for performance evaluation. We assumed that all controlled variables can be measured in real

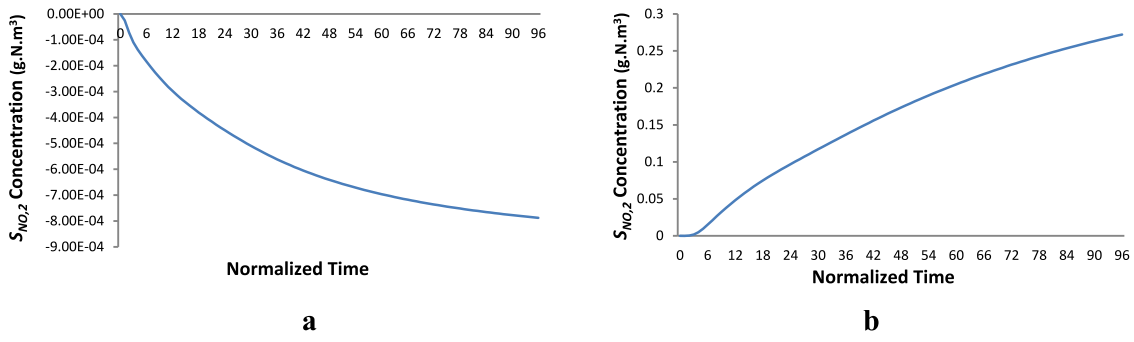

Fig. 7. $S_{NO,2}$ step responses to influent flow rate (a) and influent ammonium concentration (b).

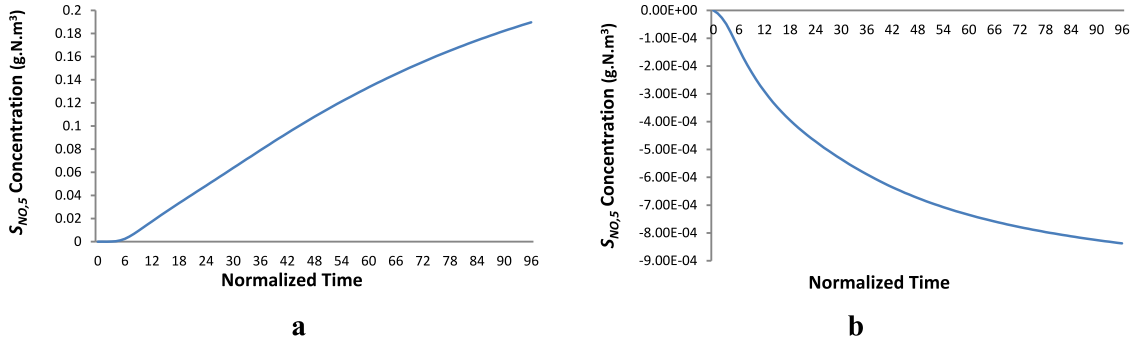

Fig. 8. $S_{NO,5}$ step responses to influent flow rate (a) and influent ammonium concentration (b).

Table 9
Tuning parameters in DMC/EDMC configurations.

Weight matrix Q	Weight matrix R	R_1	R_2	w_1	w_2	ρ_{min}	ρ_{max}
$\begin{bmatrix} 10^0 & 0 & 0 \\ 0 & 10^0 & 0 \\ 0 & 0 & 10^0 \end{bmatrix}$	$\begin{bmatrix} 10^{-3} & 0 \\ 0 & 10^{-3} \end{bmatrix}$	1	0.1	1	80	10	10

time. To this end, B_0 class sensors, with measurement range [0-20], were incorporated in the simulation environment for measuring $S_{NH,5}$, $S_{NO,5}$ and $S_{NO,2}$. All simulations were performed in the Matlab/Simulink® programming environment. The DMC and EDMC optimization problems were formulated using the Yalmip® [28] toolbox, and were solved with the GUROBI® 9.0 solver (academic license), using a machine with an Intel® core™ i7-5500U @ 2.4 GHz processor, 8.00 GB RAM, and Windows® 10 operating system.

5.3.1. DMC and EDMC results for the dry weather influent profile

In this section the results of the DMC and EDMC control schemes are presented, in the case of the dry weather influent profile. The results are summarized and compared with the default PI control strategy of the BSM1 model in Tables 10–11. All performance indexes have been defined previously in Section 4 and have been computed based on the 7-days evaluation period.

The results display that the EDMC control configurations managed to satisfy the objective of reducing the energy consumption of the WWTP, since the respective *CI* and *OCI* index values are considerably lower compared to the DMC designs and to the default PI control strategy. This is achieved at the expense of a higher *EQ* index compared to DMC designs, but in the case of the EDMC_3by2_96 design, the *EQ* index is practically no worse compared to the default PI strategy. The DMC controllers clearly outperformed the EDMC designs and the default BSM1 control scheme with respect to the *EQ* index. The difference in the performances regarding the *EQ* index is mainly due to the longer period of violating the upper ammonia nitrogen effluent constraint in the case of EDMC, which is the result of the decreased aeration energy consumption. On the other hand, violation periods of the total effluent nitrogen concentration constraint were very similar between the DMC and EDMC designs (with the exception of the aggressive EDMC_3by2_96 controller), but considerably lower compared to the default PI strategy, as a consequence of the upper limits imposed on the $S_{NO,5}$ controlled variable in the formulation of the DMC and EDMC optimization problems. The performances of the DMC and EDMC configurations were compared further by selecting DMC_3by2_48 between the two DMC designs, as it corresponds to the lowest *CI* and *EQ* index values, and the EDMC_3by2_96 controller between the two EDMC designs.

Fig. 10 portrays the responses of the controlled variables $S_{NH,5}$, $S_{NO,5}$, $S_{NO,2}$ and the effluent concentrations $S_{NH,eff}$ and TN_{eff} corresponding to the EDMC_3by2_96 and DMC_3by2_48 controllers, along with the upper and lower limits, and compares them with the default PI scheme, while Fig. 11 presents the respective trajectories of the manipulated variables. The responses are presented only for the 9th simulation day, so that the differences between the control schemes can be observed clearly. Similar responses have been obtained for the rest of the simulation periods. The lower bound for $S_{NO,2}$ and the upper limit value of $S_{NO,5}$ were selected by the EDMC_3by2_96 controller as the most economic working points of the system, while significant violations are observed only with respect to the upper bound on $S_{NH,5}$. The DMC_3by2_48 controller tries to maintain the controlled variables near the setpoints, but this leads to fluctuations between the lower and the upper bounds for the controlled variable

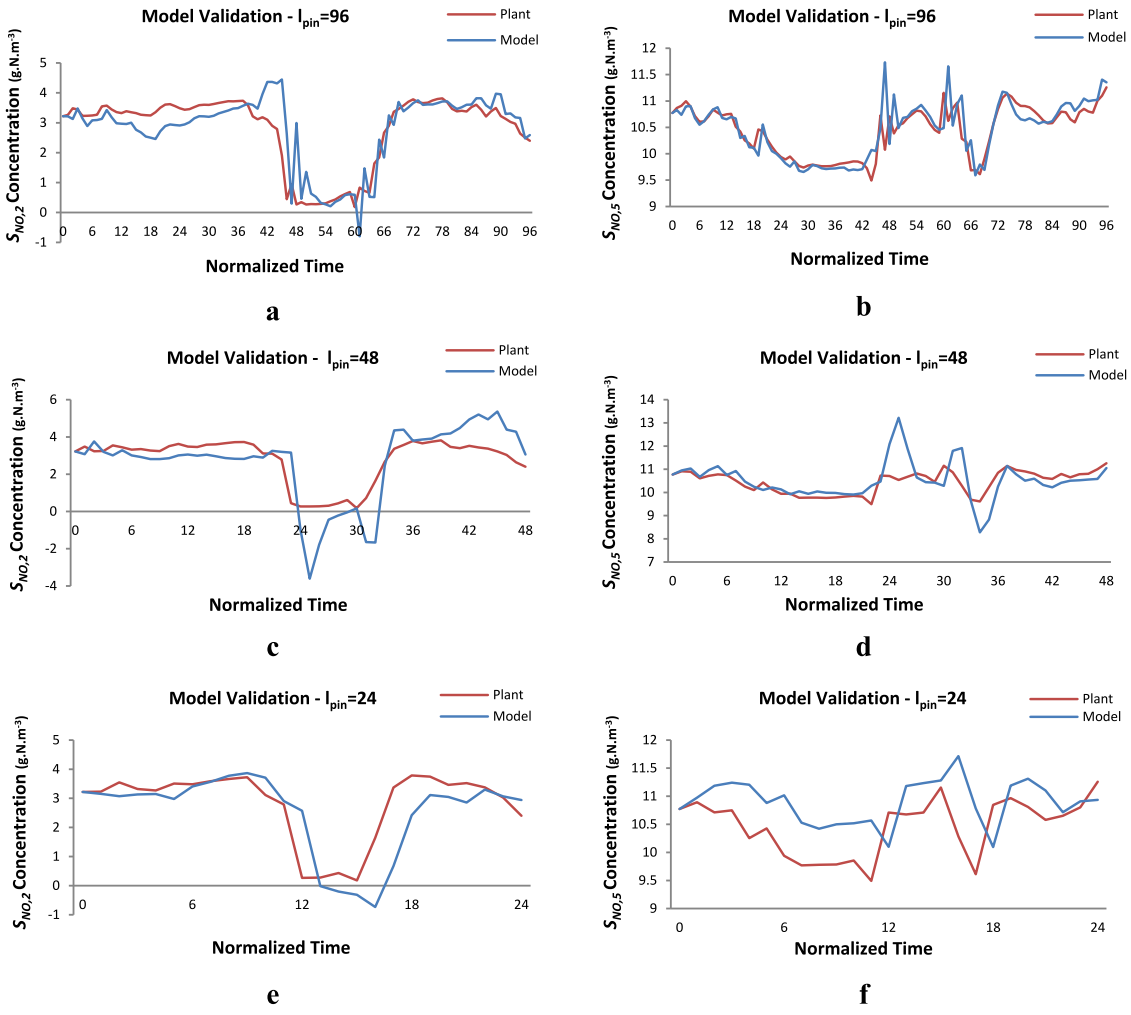

Fig. 9. Actual plant responses and step response model predictions for controlled variables $S_{NO,2}$ and $S_{NO,5}$.

Table 10
Simulation results for the DMC and EDMC control schemes. Also the results of the default BSM1 control strategy are presented.

Controller type	$\bar{S}_{NH,eff}$ (g N m^{-3})	$\bar{S}_{NO,eff}$ (g N m^{-3})	$\bar{S}_{NH,eff}+\bar{S}_{NO,eff}$ (g N m^{-3})	AE_5 (kWh d^{-1})	PE_{Q_a} (kWh d^{-1})	EQ (kg d^{-1})	EQ[a] (%)	CI (kWh d^{-1})	CI[a] (%)	OCI (kWh d^{-1})	OCI[a] (%)
Default_PI	2.54	12.42	14.96	854.39	74.23	6123.23	–	928.62	–	16 382.19	–
DMC_3by2 _48	2.90	10.65	13.55	707.15	179.70	6004.73	−1.94	886.86	−4.51	16 347.48	−0.21
DMC_3by2 _96	2.96	10.57	13.53	734.97	171.88	6026.41	−1.58	906.85	−2.35	16 364.40	−0.11
EDMC_3by2_48	3.11	12.13	15.23	693.59	64.42	6388.86	4.34	758.01	−18.38	16 216.53	−1.01
EDMC_3by2_96	3.03	10.97	14.00	737.99	94.13	6131.22	0.13	832.12	−10.40	16 289.71	−0.56

[a]EQ, CI and OCI percentages represent deviations from Default_PI. Negative values denote decrease, while positive value denote increase of the respective metric.

Table 11
Effluent violation periods of the DMC and EDMC control schemes and the default BSM1 control strategy.

Controller type	$TN_{eff,viol}$ (days)	$TN_{eff,viol}$ (%)	$S_{NH,eff,viol}$ (days)	$S_{NH,eff,viol}$ (%)
Default_PI	1.28	18.30	1.20	17.11
DMC_3by2 _48	0.95	13.54	1.13	16.07
DMC_3by2 _96	0.90	12.80	1.18	16.82
EDMC_3by2_48	2.23	31.85	1.94	27.68
EDMC_3by2_96	0.93	13.24	1.45	20.68

$S_{NO,2}$. The DMC_3by2_48 controller produces the lowest effluent concentrations among the three controllers, as expected from the previous analysis. On the other hand, the EDMC_3by2_96 controller aims at driving the manipulated variables at their lower bounds, which corresponds to a lower energy cost. This is achieved by making the input trajectories more aggressive, but given the long sampling period of 15 min, these trajectories can be realized by the actuators in a real-life operation.

Table 12 depicts the computational times required to perform the complete DMC and EDMC simulations, which span both the stabilization and the evaluation periods. The computational times are comparable and illustrate that the substitution of the classical quadratic objective by the linear economic function in the proposed EDMC scheme does not affect the performance of the controller with respect to the computational effort required to solve on-line the optimal control problem.

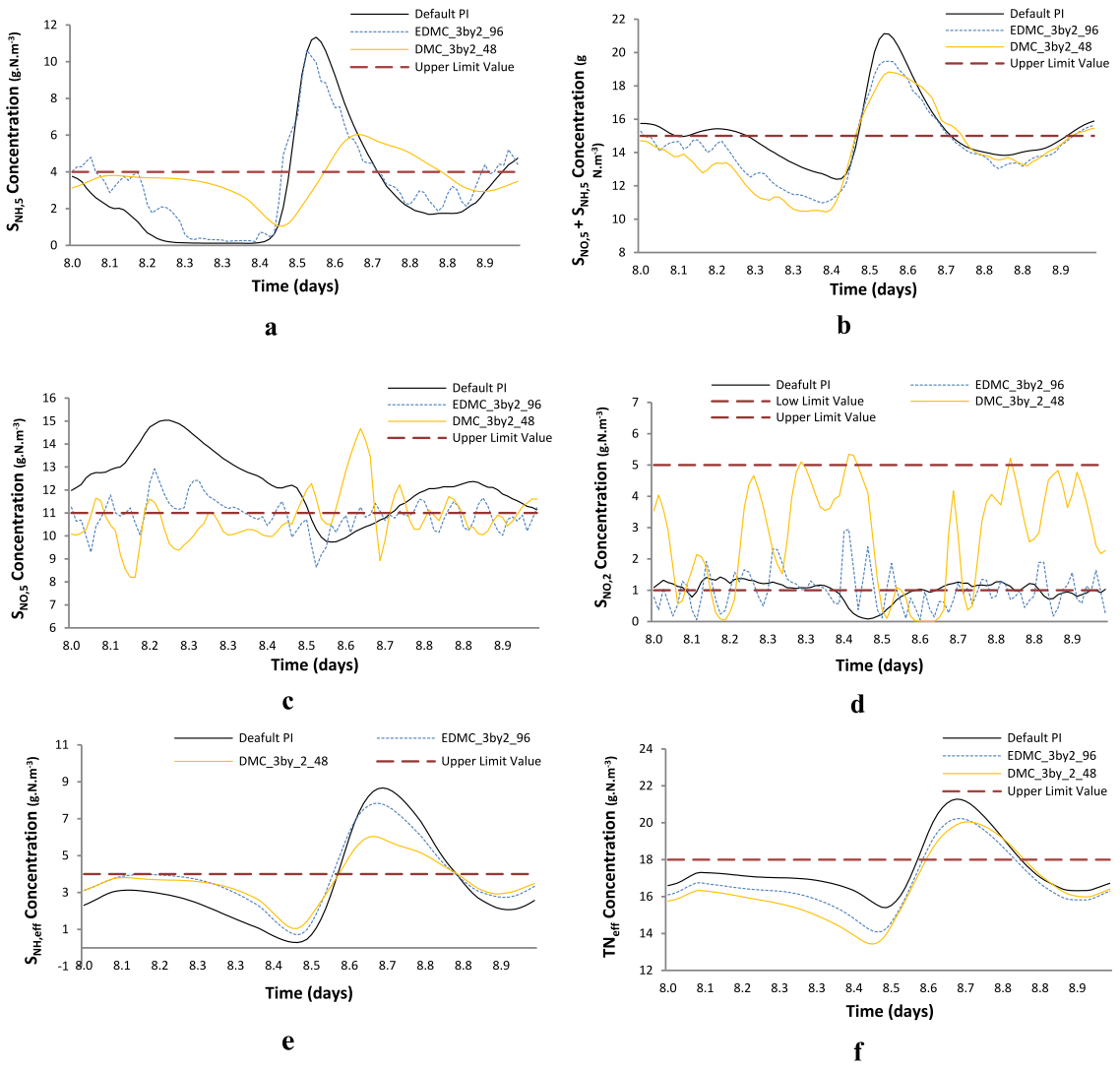

Fig. 10. Trajectories of $S_{NH,5}$ (a), $S_{NH,5}$ + $S_{NO,5}$ (b), $S_{NO,5}$ (c), $S_{NO,2}$ (d), $S_{NH,eff}$ (e) and TN_{eff} (f) of EDMC_3by_2_96 and DMC_3by2_48 control schemes during the 9th day of simulation compared with the default BSM1 PI control strategy.

Table 12
Computational times for a fourteen-day simulation.

Controller type	*Time* (s)
DMC_3by2 _48	595.33
DMC_3by2 _96	1155.70
EDMC_3by2 _48	676.81
EDMC_3by2 _96	1393.90

5.3.2. EDMC results under uncertainty in future predictions of measured disturbances

In Section 5.3.1, future predictions of measured disturbances along the prediction horizon were assumed perfectly known. In real-life situation, though, this is not the case. This subsection examines the performance of the EDMC controllers when uncertainty is introduced in future predictions of the measured disturbances in the form of white noise, i.e. time series with zero mean value and constant variance, equal to 8 g N m^3 and 8000 m^3 d^{-1} for $S_{NH,in}$ and Q_a, respectively. Fig. 12 presents the profiles of the two measured disturbances in the original BSM1 model and when uncertainty is introduced.

Table 13, presents the results of the proposed EDMC control scheme, when uncertainty on future predictions for measured disturbances is taken into consideration. The obtained results show that there are no major differences compared to the results in Table 10, where perfect predictions of measured disturbances were assumed. In fact, lower *CI* and *OCI* index values were obtained at the cost of a slight deterioration of the *EQ* index.

5.3.3. EDMC results for different influent profiles

In order to evaluate the robust performance of the proposed EDMC methods, the controllers designed in Section 5.3, were tested on influent profiles for storm and rain weather conditions, without performing any modifications on the predictive models, or in the selection of the tuning parameters. The results are summarized in Tables 14 and 15 and compared with the respective results of the DMC control scheme.

In the case of the storm influent profile, the *CI* index was improved considerably by the EDMC_3by2_48 controller in comparison to the default BSM1 PI strategy, at the cost of a much higher *EQ* index. In the case of the rain influent profile, the EDMC controllers did not manage to outperform the default control strategy. The results are still acceptable but indicate that the performance of the EDMC controllers can be improved if the predictive models and the EDMC tuning parameters are adjusted to the specific operating conditions imposed by this weather profile. Comparison with the results of the DMC control schemes gave similar outcomes with the ones presented before for the

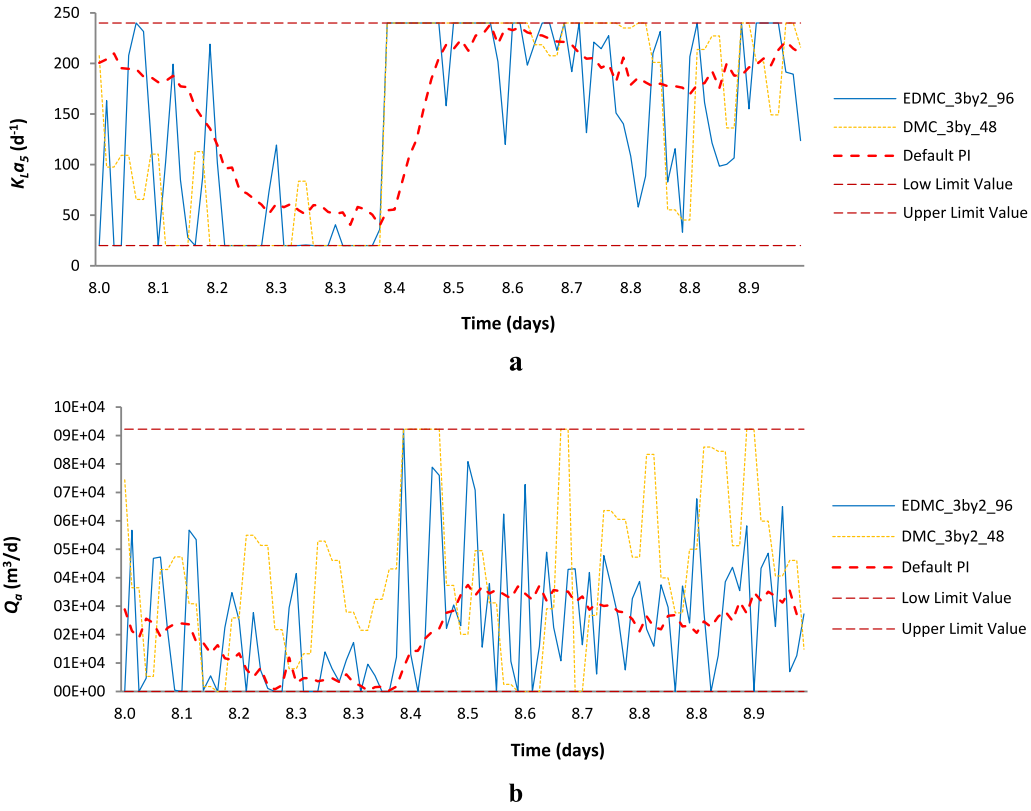

Fig. 11. Trajectories of the manipulated inputs $K_L a_5$ (a) and Q_a (b) for the default PI control strategy (red dashed line) and the EDMC_3by2_96 (blue solid line) during the 9th day of simulation.

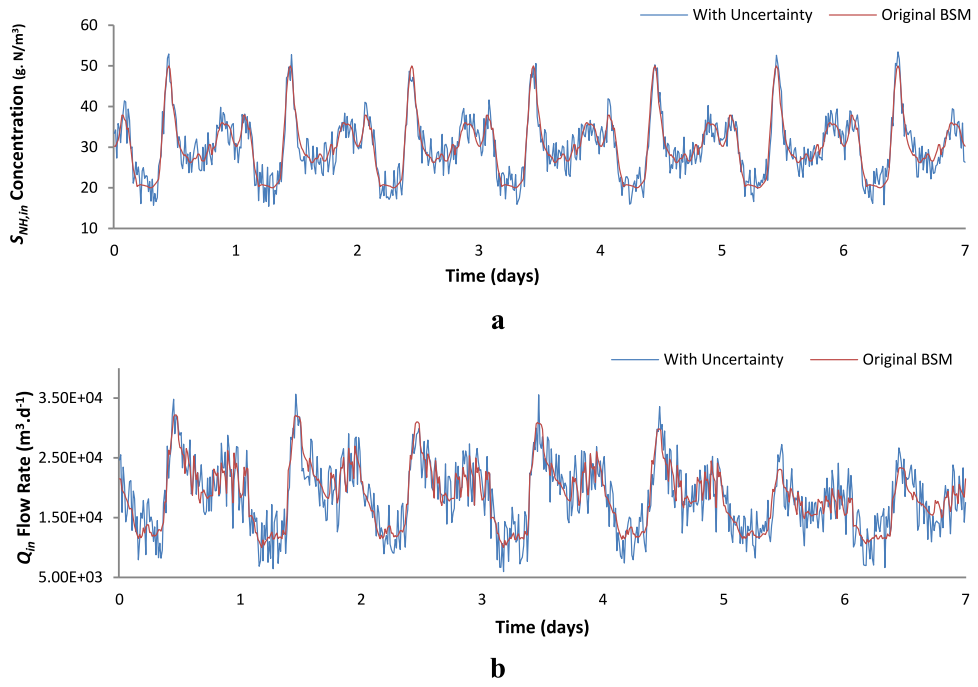

Fig. 12. Influent profiles with uncertainty (red line) and without uncertainty (blue line) for disturbances $S_{NH,in}$ (a), and Q_{in} (b).

Table 13
Simulation results for the EDMC control strategy with measured disturbances under uncertainty. Also, the results of the default BSM1 control strategy are presented.

Controller type	$\bar{S}_{NH,eff}$ (g N m^{-3})	$\bar{S}_{NO,eff}$ (g N m^{-3})	$\bar{S}_{NH,eff}+\bar{S}_{NO,eff}$ (g N m^{-3})	AE_5 (kWh d^{-1})	PE_{Q_a} (kWh d^{-1})	EQ (kg d^{-1})	EQ[a] (%)	CI (kWh d^{-1})	CI[a] (%)	OCI (kWh d^{-1})	OCI[a] (%)
Default_PI	2.54	12.42	14.96	854.39	74.23	6123.23	–	928.62	–	16 382.19	–
EDMC_3by2_48	3.35	12.09	15.45	670.64	60.47	6518.29	6.45	731.11	−21.18	16 183.51	−1.21
EDMC_3by2_96	3.06	10.92	13.99	734.87	95.86	6142.77	0.32	830.73	−10.55	16 283.06	−0.61

[a]EQ, CI and OCI percentages represent deviations from Default_PI. Negative values denote decrease, while positive value denote increase of the respective metric.

Table 14
Simulation results for the DMC and EDMC control strategies for the storm weather influent profile. Also the results of the default BSM1 control strategy are given.

Controller type	$\bar{S}_{NH,eff}$ (g N m^{-3})	$\bar{S}_{NO,eff}$ (g N m^{-3})	$\bar{S}_{NH,eff}+\bar{S}_{NO,eff}$ (g N m^{-3})	AE_5 (kWh d^{-1})	PE_{Q_a} (kWh d^{-1})	EQ (kg d^{-1})	EQ[a] (%)	CI (kWh d^{-1})	CI[a] (%)	OCI (kWh d^{-1})	OCI[a] (%)
Default_PI	3.06	10.52	13.58	874.31	99.66	7211.91	–	973.97	–	17 252.90	–
DMC_3by2 _48	3.11	9.78	12.89	865.25	191.18	7092.75	−1.65	1056.43	8.47	17 382.32	0.75
DMC_3by2 _96	3.14	9.69	12.83	904.50	184.16	7094.13	−1.63	1088.66	11.77	17 433.50	1.05
EDMC_3by2_48	3.67	11.11	14.78	784.31	56.28	7727.24	7.15	840.59	−13.70	17 130.74	−0.71
EDMC_3by2_96	3.27	9.88	13.15	870.42	105.71	7209.32	−0.04	976.13	0.22	17 261.87	0.05

[a]EQ, CI and OCI percentages represent deviations from Default_PI. Negative values denote decrease, while positive value denote increase of the respective metric.

Table 15
Simulation results for the DMC and EDMC control strategies for the rain weather influent profile. Also the results of the default BSM1 control strategy are given.

Controller type	$\bar{S}_{NH,eff}$ (g N m^{-3})	$\bar{S}_{NO,eff}$ (g N m^{-3})	$\bar{S}_{NH,eff}+\bar{S}_{NO,eff}$ (g N m^{-3})	AE_5 (kWh d^{-1})	PE_{Q_a} (kWh d^{-1})	EQ (kg d^{-1})	EQ[a] (%)	CI (kWh d^{-1})	CI[a] (%)	OCI (kWh d^{-1})	OCI[a] (%)
Default_PI	3.22	9.14	12.36	825.81	120.40	8174.99	–	946.21	–	15 984.85	–
DMC_3by2 _48	3.20	8.72	11.92	955.88	217.40	8055.41	−1.46	1173.28	24.00	16 247.15	1.64
DMC_3by2 _96	3.24	8.70	11.94	970.55	207.99	8082.54	−1.13	1178.53	24.55	16 269.18	1.78
EDMC_3by2_48	3.41	9.87	13.27	915.73	77.29	8488.80	3.84	993.02	4.95	16 041.25	0.35
EDMC_3by2_96	3.28	8.77	12.06	940.38	123.13	8130.62	−0.54	1063.51	12.40	16 106.61	0.76

[a]EQ, CI and OCI percentages represent deviations from Default_PI. Negative values denote decrease, while positive value denote increase of the respective metric

Table 16
Results of the EMPC controllers proposed by Zeng and Liu [16] for the dry influent profile, the default PI controller and the proposed EDMC controllers.

Controller type	$\bar{S}_{NH,eff}$ (g N m^{-3})	AE_5 (kWh d^{-1})	PE_{Q_a} (kWh d^{-1})	EQ (kg d^{-1})	EQ[a] (%)	CI (kWh d^{-1})	CI[a] (%)	OCI (kWh d^{-1})	OCI[a] (%)
Default PI	2.54	854.39	74.23	6123.23	–	928.62	–	16 382.19	–
Zeng&Liu_EQ	2.12	847.00	140.19	5671.86	−7.37	987.19	6.30	16 493.88	0.68
Zeng&Liu_EQ_OCI	2.30	715.78	143.42	5693.64	−7.02	859.19	−7.49	16 361.50	−0.13
EDMC_3by2_48	3.41	693.59	64.42	6388.86	4.34	758.01	−18.38	16 216.53	−1.01
EDMC_3by2_96	3.28	737.99	94.13	6131.22	0.13	832.11	−10.40	16 289.71	−0.56

[a]EQ, CI and OCI percentages represent deviations from Default_PI. Negative values denote decrease, while positive value denote increase of the respective metric

dry weather simulations. DMC improved the EQ index, but the CI index values were considerably higher.

5.3.4. Comparison to alternative EMPC control strategies

In this section the results of the proposed EDMC under the dry influent profile, are compared to alternative EMPC strategies that have been presented in the literature. First, the EMPC controller proposed by Zeng&Liu [16], was considered. This configuration assumes perfect match between the predictive model and the actual dynamics of the process, and further assumes that the full state vector consisting of 145 state variables, can be measured in real time. Furthermore, the full *EQ* (Eq. (4.1)) and *OCI* (Eq. (4.3)) indices were used in the objective function: Zeng&Liu_EQ stands for the control formulation where only the *EQ* was taken into consideration, while Zeng&Liu_EQ_OCI represents the case where both the aforementioned terms are part of the objective function. The results are summarized in Table 16. The Zeng&Liu_EQ controller achieved a significant reduction of 7.37% in the *EQ* index, with respect to the default PI. Therefore, this particular controller defines the limitations on the performance an economic oriented control strategy can achieve, as far as the *EQ* index is concerned. The EDMC controllers proposed in the current paper clearly outperformed the ones designed in [16] in terms of the *CI* index, while the *EQ* index was maintained at an acceptable level.

In Revollar et al. [18], a reduced order nonlinear model of the BSM1 was used for prediction purposes, while perfect measurement of the full state and perfect knowledge of the future evolution of the disturbances was considered. Two economic control formulations were developed, namely a purely Economic MPC (EMPC) and a Hybrid Economic MPC (HEMPC). In the first formulation, the cost function included only economic oriented terms, while in the latter a tracking term was also included in the objective function of the optimization problem. Both control formulations were further divided into subcategories according to the economic terms included in the cost function. OCI refers to the case where only operation costs are present in the economic oriented term. NH takes additionally into consideration fines on effluent ammonia concentration and OCI+NH refers to the case where both the terms are present in the economic oriented term of the cost function. For further details on the formulation of these economic oriented control schemes the reader is referred to the original paper [18]. Table 17 summarizes the results of Ref. [18], which were obtained based on a 4-day simulation period and compares them with the default PI control strategy.

For comparison purposes the EDMC controllers designed in the current paper were simulated during the same 4-day period, i.e. between the eighth and the twelfth day. The results are also presented in Table 17 and illustrate that the proposed EDMC

Table 17
Results of the EMPC and HEMPC controllers proposed by Revollar et al. [18] and the 4-day simulation results under the dry influent profile of the default PI controller and the proposed EDMC controllers. Also, the influent quality index of each control strategy is provided.

Controller type	IQ (kg d^{-1})	$\bar{S}_{NH,eff}$ (g N m^{-3})	AE_5 (kWh d^{-1})	PE_{Q_a} (kWh d^{-1})	EQ (kg d^{-1})	EQ[a] (%)	CI (kWh d^{-1})	CI[a] (%)	OCI (kWh d^{-1})	OCI[a] (%)
4-day default PI	56 050.43	3.08	935.01	85.13	6686.38	–	1020.14	–	18 113	–
Revollar_HEMPC-OCI	55 945.14	3.21	958.27	109.78	6783.9	1.46	1068.05	4.70	18 021	−0.51
Revollar_HEMPC-OCI + NH	55 945.14	2.74	986.27	79.98	6584.7	−1.52	1066.25	4.52	18 052	−0.34
Revollar_HEMPC-NH	55 945.14	2.55	1011.27	58.06	6698.0	0.13	1069.33	4.82	18 064	−0.27
Revollar_EMPC-OCI	55 945.14	6.05	466.27	39.26	8289	23.97	505.53	−50.45	17 466	−3.57
Revollar_EMPC-OCI + NH	55 945.14	3.47	997.27	0.382	7617.0	13.92	997.65	−2.21	17 988	−0.69
Revollar_EMPC-NH	55 945.14	2.37	1433.27	0	7315.3	9.41	1433.27	40.50	18 434	1.77
4-day EDMC_3by2_48	56 050.43	3.51	789.88	60.90	7031.95	5.17	850.78	−16.60	17 954	−0.88
4-day EDMC_3by2_96	56 050.43	3.55	832.36	101.32	6745.81	0.89	933.68	−8.48	17 994	−0.65

[a]EQ, CI and OCI percentages represent deviations from Default_PI. Negative values denote decrease, while positive value denote increase of the respective metric.

schemes outperformed almost all controllers presented in [18] in terms of the *CI* index, while the *EQ* index was only slightly higher compared to the default PI. More specifically, the lowest *CI* value was achieved by EDMC_3by2_48, at the cost of 5.17% increase of the *EQ* index over the default PI strategy. The EMPC-OCI controller design in [18], produced a very low *CI* index, but the corresponding *EQ* value was unacceptably high. Finally, the *OCI* value achieved by the proposed economic oriented control strategies was lower compared to all economic oriented control strategies proposed in [18] with the exception again of the EMPC-OCI controller.

6. Conclusion

In this paper novel EDMC strategies were developed for the control of WWTPs. The proposed schemes combine the simplicity of the traditional DMC controllers with the advantages of the recently proposed EMPC approaches. The main objective of the linear optimization problem formulated at each time instant is the reduction of the energy consumption, and more specifically the decrease of the costs associated with the aeration of the last aerobic compartment and the internal recirculation flow rate. The composition of the effluent is also taken into consideration in the form of penalties for off-specification operation.

The proposed EDMC schemes were compared to conventional DMC approaches, to the default PI strategy and to other EMPC configurations proposed in the literature. The results demonstrated that the proposed control configurations clearly surpass the default control strategy and the conventional DMC methods in terms of reducing the energy cost and are comparable to other EMPC approaches. The most important advantage of the proposed method is that it can be adapted and applied to real-life implementations, because it relies on models derived from step tests, which are easily implementable in real WWTPs. Furthermore, only minimal information from the process is required in real time, for formulating and solving a computationally tractable EDMC optimization problem.

Our plans for extending the proposed method include the development of an EDMC approach based on nonlinear machine learning models, that will be trained on data collected from the real plant. We are also planning to investigate how the proposed EDMC approach can be adjusted to other process control problems, where the cost function might be nonlinear with respect to the decision variables. Both extensions will lead to the development of nonlinear EMPC strategies, which will be compared against the EDMC approach presented in the current manuscript in terms of performance and computational complexity.

Declaration of competing interest

The authors declare that they have no known competing financial interests or personal relationships that could have appeared to influence the work reported in this paper.

Acknowledgments

This research has been co-financed by the European Regional Development Fund of the European Union and Greek national funds through the Operational Program Competitiveness, Entrepreneurship and Innovation, under the call RESEARCH – CREATE – INNOVATE (project code: T2EΔK-02191).

References

[1] A. Iratni, N. Bin Chang, Advances in control technologies for wastewater treatment processes: Status, challenges, and perspectives, IEEE/CAA J. Autom. Sin. 6 (2019) 337–363, http://dx.doi.org/10.1109/JAS.2019.1911372.
[2] D. Rosso, L.E. Larson, M.K. Stenstrom, Aeration of large-scale municipal wastewater treatment plants: State of the art, Water Sci. Technol. 57 (2008) 973–978, http://dx.doi.org/10.2166/wst.2008.218.
[3] V.C. Machado, D. Gabriel, J. Lafuente, J.A. Baeza, Cost and effluent quality controllers design based on the relative gain array for a nutrient removal WWTP, Water Res. 43 (2009) 5129–5141, http://dx.doi.org/10.1016/j.watres.2009.08.011.
[4] A.C.B. De Araújo, S. Gallani, M. Mulas, G. Olsson, Systematic approach to the design of operation and control policies in activated sludge systems, Ind. Eng. Chem. Res. 50 (2011) 8542–8557, http://dx.doi.org/10.1021/ie101703s.
[5] A. Stare, D. Vrečko, N. Hvala, S. Strmčnik, Comparison of control strategies for nitrogen removal in an activated sludge process in terms of operating costs: A simulation study, Water Res. 41 (2007) 2004–2014, http://dx.doi.org/10.1016/j.watres.2007.01.029.
[6] B. Vivekanandan, A.S. Rao, Comparison of MPC and PI control strategies for activated sludge process, 238 (2016) 230–238.
[7] M. Francisco, P. Vega, S. Revollar, Model predictive control of BSM1 benchmark of wastewater treatment process: A tuning procedure, in: Proc. IEEE Conf. Decis. Control., 2011, pp. 7057–7062, http://dx.doi.org/10.1109/CDC.2011.6160378.
[8] W. Shen, X. Chen, M.N. Pons, J.P. Corriou, Model predictive control for wastewater treatment process with feedforward compensation, Chem. Eng. J. 155 (2009) 161–174, http://dx.doi.org/10.1016/j.cej.2009.07.039.
[9] M. O'Brien, J. Mack, B. Lennox, D. Lovett, A. Wall, Model predictive control of an activated sludge process: A case study, Control Eng. Pract. 19 (2011) 54–61, http://dx.doi.org/10.1016/j.conengprac.2010.09.001.
[10] P. Vega, S. Revollar, M. Francisco, J.M. Martín, Integration of set point optimization techniques into nonlinear MPC for improving the operation of WWTPs, Comput. Chem. Eng. 68 (2014) 78–95, http://dx.doi.org/10.1016/j.compchemeng.2014.03.027.
[11] M. Ellis, H. Durand, P.D. Christofides, A tutorial review of economic model predictive control methods, J. Process Control. 24 (2014) 1156–1178, http://dx.doi.org/10.1016/j.jprocont.2014.03.010.
[12] J.B. Rawlings, D. Angeli, C.N. Bates, Fundamentals of economic model predictive control, in: Proc. IEEE Conf. Decis. Control., 2012, pp. 3851–3861, http://dx.doi.org/10.1109/CDC.2012.6425822.
[13] R. Moliner-Heredia, I. Penarrocha-Alos, R. Sanchis-Llopis, Economic model predictive control of wastewater treatment plants based on BSM1 using linear prediction models, in: IEEE Int. Conf. Control Autom. ICCA. 2019-, 2019, pp. 73–78, http://dx.doi.org/10.1109/ICCA.2019.8899974.
[14] H. Durand, M. Ellis, P.D. Christofides, Economic model predictive control designs for input rate-of-change constraint handling and guaranteed economic performance, Comput. Chem. Eng. 92 (2016) 18–36, http://dx.doi.org/10.1016/j.compchemeng.2016.04.026.
[15] M. Henze, C.P. Leslie Grady Jr., W. Gujer, G.V.R. Marais, T. Matsuo, Activated sludge model (1) by IAWPRC, 1986.

[16] J. Zeng, J. Liu, Economic model predictive control of wastewater treatment processes, Ind. Eng. Chem. Res. 54 (2015) 5710–5721, http://dx.doi.org/10.1021/ie504995n.
[17] O. Barrou, A. Karama, E.K. Lakhal, O. Bernard, M.N. Pons, J.P. Corriou, Estimation of a reduced model of the BSM1 activated sludge wastewater treatment plant, Int. J. Chem. React. Eng. 6 (2008) http://dx.doi.org/10.2202/1542-6580.1627.
[18] S. Revollar, P. Vega, R. Vilanova, M. Francisco, Optimal control of wastewater treatment plants using economic-oriented model predictive dynamic strategies, Appl. Sci. 7 (2017) http://dx.doi.org/10.3390/app7080813.
[19] J. Alex, L. Benedetti, J. Copp, K.V. Gernaey, U. Jeppsson, I. Nopens, M.-N. Pons, L. Rieger, C. Rosen, J.P. Steyer, P. Vanrolleghem, S. Winkler, I.E.V. Magdeburg, G.L. Benedetti, Benchmark simulation model (1) (BSM1) benchmark simulation model (1) (BSM1) contributors, Benchmark Simul. Model. 1 (2008) 1–58.
[20] Benchmarking – modelling & integrated assessment, (n.d.), 2020, http://iwa-mia.org/benchmarking/ (accessed August 14, 2020).
[21] J. Richalet, A. Rault, J.L. Testud, J. Papon, Model predictive heuristic control. Applications to industrial processes, Automatica 14 (1978) 413–428, http://dx.doi.org/10.1016/0005-1098(78)90001-8.
[22] C.R. Cutler, B.L. Ramaker, Dynamic matrix control - a computer control algorithm., J. Environ. Sci. Heal. Part B Pestic. Food Contam. Agric. Wastes. 1 (1979) http://dx.doi.org/10.1109/JACC.1980.4232009.
[23] E.F. Camacho, C. Bordons Alba, Model predictive control, 2007.
[24] J. Maciejowski, Predictive control with constraints, 2002.
[25] M. Mulholland, Applied Process Control Essential Methods, Wiley-VCH, 2016.
[26] J. Maciejowski, E. Kerrigan, Soft constrains and exact penalty functions in model predictive control, predict. Control, 2000, pp. 1–290, http://dx.doi.org/10.1142/9789814343305_0012.
[27] P. Samuelsson, B. Halvarsson, B. Carlsson, Cost-efficient operation of a denitrifying activated sludge process, Water Res. 41 (2007) 2325–2332, http://dx.doi.org/10.1016/j.watres.2006.10.031.
[28] J. Lofberg, YALMIP : a toolbox for modeling and optimization in MATLAB, 2005, pp. 284–289, http://dx.doi.org/10.1109/cacsd.2004.1393890.